# The SAF on Climate Monitoring: Cloud Products

K.-G. Karlsson

## 1 Introduction

Clouds play an important role in the climate system due to their strong interaction with radiation processes and because of being an important component of the global hydrological cycle. The latter circumstance also means that there is a direct link between clouds and the most important greenhouse gas - atmospheric water vapour. Consequently, a climate monitoring program must also include the monitoring of clouds.

Satellite systems, acting as observational platforms, offer cloud observations that in many ways are superior to most ground based observations. Most obvious is the ability to observe large areas with high spatial and temporal resolution. In addition, the fact that satellites are able to monitor the effective radiative impact at the top of the atmosphere (e.g., the cloud-related contribution to the planetary albedo) makes satellite cloud observations crucial for understanding the planetary (i.e., earth plus the atmosphere) radiation balance. A third important factor is that measurements of cloud properties from space are also important for understanding radiation conditions at the earth surface (the surface radiation balance). However, complementary surface observations are necessary here since it is generally impossible to infer conditions below thick clouds from satellite measurements.

To cover the various aspects of clouds and their impact on radiation conditions, the EUMETSAT Climate Monitoring SAF (CM-SAF) has a Clouds programme for the extraction of climate-relevant cloud parameters. State-of-the-art cloud algorithms are used which are further adapted and developed for the climate monitoring purpose. This paper gives an overview of these cloud products. Section 2 gives a general introduction to the products, the used satellite data sources and the applicable geographic processing domain. Section 3 describes each product in detail and the concluding section 4 presents the plans for the future.

## 2 CM-SAF cloud products and satellite data sources

Table 1 below lists the current six CM-SAF cloud products and their spatial and temporal resolution.

These products are produced from satellite imagery from the AVHRR instrument on the polar orbiting NOAA satellites (from January 2005) and from the SEVIRI sensor onboard the Meteosat Second Generation (MSG) satellites (introduced later in the second half of 2005). All product examples shown below in this paper are derived from NOAA AVHRR data.

**Table 1** Overview of CM-SAF cloud products and their spatial and temporal resolution.

| Product | Acronym | Resolution | | | | |
|---|---|---|---|---|---|---|
| | | Spatial | Temporal | | | |
| | | | Daily | Weekly | Monthly | MMDC (Monthly Mean Diurnal Cycle) |
| Fractional cloud cover | CFC | 15 km | ✓ | | ✓ | ✓[1] |
| Cloud type | CTY | 15 km | ✓ | | ✓ | ✓[1] |
| Cloud top temperature, height, and pressure | CTT, CTH, CTP | 15 km | ✓ | | ✓ | ✓[1] |
| Cloud phase | CPH | 15 km | ✓ | | ✓ | ✓ |
| Cloud optical thickness | COT | 15 km | ✓ | | ✓ | ✓[1] |
| Cloud water path | CWP | 15 km | ✓ | | ✓ | ✓[1] |
| [1]: monthly mean diurnal cycle will be derived only for products extracted from MSG data | | | | | | |

The geographical domain is described in Figure 1. In the first production phase (see section 4 for information on future production phases) the products are produced over the CM-SAF Baseline Area. This area covers the region between longitudes 60°W and 60°E and latitudes between 30°N and 80°N. Thus, the European area plus large parts of the North Atlantic, Greenland and the Arctic Sea is covered. Also parts of northern Africa and the Middle East region is covered.

To enable data representation in an equal area grid resolution of 15 km the final products are defined in a sinusoidal projection which is described in Figure 2.


**Figure 1** CM-SAF coverage area and subareas

# 3 Detailed product and algorithm descriptions

## *3.1 Fractional Cloud Cover (CFC)*

Derived directly from the results of the Cloud Mask (CM) product, the fractional cloud cover (CFC) is defined as the fraction of cloudy pixels per sub-region compared to the total number of analysed pixels in the sub-region. That is to say, fractional cloud cover is computed as the fraction of all pixels within a 15x15 km grid square that has been classified as either cloud-filled or cloud contaminated. Fractional cloud cover is expressed in percent.

This product is calculated using the SAFNWC cloud mask algorithms (see http://nwcsaf.inm.es/ for details on the SAFNWC project). The algorithm applied to NOAA AVHRR data is described in detail by Dybbroe et al. (2005) and the corresponding algorithm applied to MSG SEVIRI data is described by Derrien and LeGleau (2003, see also http://www.meteorologie.eu.org/safnwc/.) Both CM algorithms are based on a multi-spectral thresholding technique applied to each pixel of the satellite scene. Several threshold tests may be applied (and must be passed) before a pixel is assigned to be cloudy or cloud-free (or partially cloudy). For every satellite overpass a unique set of feature thresholds is extracted in full image resolution and is applicable only for that particular satellite scene.

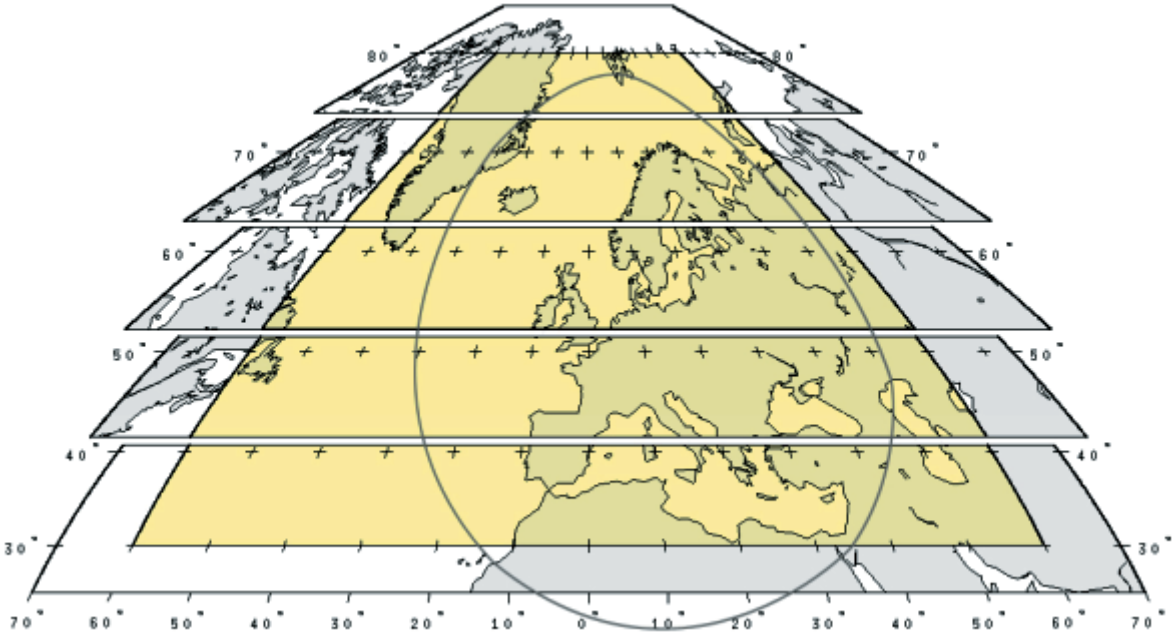


**Figure 2** The CM-SAF Baseline Area in sinusoidal projection and sliced in different sub-regions. The circle marks the area within the CM-SAF baseline area which can be seen with the local HRPT receiving station in Offenbach, Germany.

Figure 3 below gives an example of the CFC product for the month of April 2004.

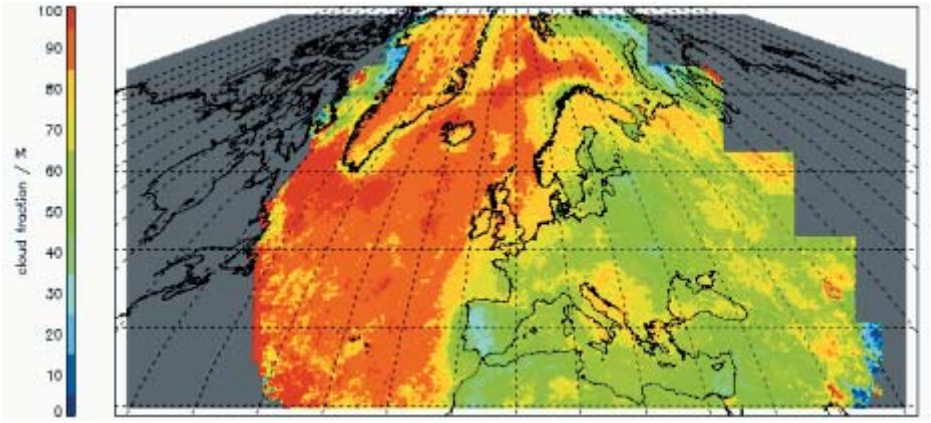


**Figure 3** Example of the CFC monthly mean product for April 2004 for the CM-SAF Baseline area.

In the present calculation of the CFC product no attempt is made to take into account for the fact that pixels labeled as being only cloud-contaminated are not totally covered by clouds. This means that the CFC values will generally overestimate cloud amounts slightly. This have been seen in validation results but the differences are normally quite small (< 5 %). It should also be emphasized that this effect is in some sense counteracted by the fact that for any cloud detection method there will also be some small residual cloudiness present for some pixels which have been declared as cloud-free.

More problematic is the fact that it is obvious from theoretical considerations that cloud detection is generally easier to accomplish over oceanic surfaces than over land surfaces. It is partly due to generally lower and less variable surface reflectance values and partly to warmer and less variable surface temperatures over ocean surfaces compared to over land. This means that we have normally better contrasts between cloudy and cloud-free areas in satellite imagery over ocean areas except in cases of sunglints. Consequently, some underestimation of cloudiness can be expected over land areas while over ocean cloud amounts may be slightly overestimated. Unfortunately, during dark and cold periods of the year the two above-mentioned defects may co-operate in creating quite large artificial land-ocean differences in the cloud amounts. It is estimated that the overestimation of cloud amounts over ocean surfaces in these cases can reach levels between 10-20 % (although being difficult to verify due to the lack of surface observations over ocean areas). Simultaneously, the corresponding underestimation of cloud amounts over land may reach 10-20 % during the cold and dark seasons (verified by observations) while it is much smaller during other seasons. Ongoing development work is trying to find ways of mitigating these inconsistencies between results over land and over ocean.

### *3.2 Cloud Type (CTY)*

Just as for the CFC product, the CTY product is based on results from the SAFNWC Cloud Type algorithms (described by the same references given previously). Also here a thresholding approach is used. The main principle used is to make use of measured cloud temperatures in the infrared for thick clouds for the vertical separation of clouds. Furthermore, ice clouds are identified using reflection characteristics at shortwave infrared channels (e.g., at 1.6, 3.7 and 3.9 µm) and thin clouds are identified

using transmission differences revealed by measurements in three infrared channels (3.7 or 3.9 µm, 11 µm and 12 µm).

The produced CTY product is based on a condensed description of cloud properties. Presently the following five cloud classes are defined: Low clouds; Mid clouds; Opaque high clouds; Thin high clouds and Fractional clouds. Thus, the CTY results are given as five individual components. The resulting average value denotes the percentage of pixels of the appropriate class relative to all cloudy pixels in each 15x15 grid.

Figure 4 gives an example of the CTY product for the contribution from the Opaque high cloud category. Notice that the current product definition gives the relative contribution to the CFC product for each cloud type category. For example, the high values over Greenland indicates that in almost 100 % of the cloudy cases (given by the CFC value in Figure 3) the clouds were of the opaque high cloud category.

From validation activities it is well known that the ability to separate different cloud types and surface types varies with seasons, illumination conditions and the satellite viewing geometry. The main limitation here is naturally the lack of visible measurements during the dark part of the day and the problem of having very cold ground temperatures during winter. In this sense, the error characteristics are closely linked to those of the CFC product (i.e., depending very much on the success of cloud detection). This generally means that the CTY results are more reliable during the warmer seasons and during daylight conditions.

Particularly difficult is the twilight period when visible and near-infrared radiances vary rapidly and very sensitively with the sun elevation. Also cloud shadows will influence cloud type assignments negatively during twilight. The same effect will also be seen during dark and very cold winter situations where cloud detection might fail because of low level clouds being trapped in strong surface temperature inversions. Finally, when thin semi-transparent cirrus clouds are superimposed over snow-covered ground the mixed signal can sometimes give rise to an erroneous output such as opaque mid-level or high-level clouds. Otherwise, snow- or ice–covered surfaces are generally efficiently separated from clouds by use of the very low reflectivities of snow in the 1.6, 3.7 and 3.9µm channels.

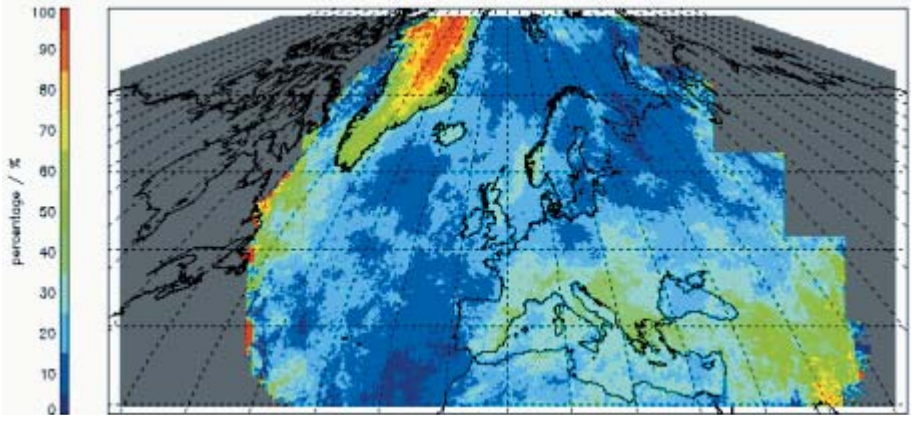


**Figure 4** Example of the CTY monthly mean product for April 2004 showing the contribution from Opaque high clouds.

*3.3 Cloud Top Temperature (CTT), Pressure (CTP) and Height (CTH)*

For the determination of cloud top information the CM-SAF is still using the SAFNWC algorithms. However, as a contrast to the situation for the cloud mask and cloud type algorithms, there are now considerable differences between the algorithms applied either to NOAA AVHRR data or MSG SEVIRI data. The reason is the availability of spectral channels in non-window regions for the SEVIRI instrument which are not present on the AVHRR instrument.

Concerning the clouds that are labelled as being opaque by the cloud type algorithm, the same technique is nevertheless used for both the AVHRR and SEVIRI methods. Radiance simulations, using the RTTOV radiative transfer model (Eyre, 1991, Saunders et al., 1999), are computed using Numerical Weather Prediction (NWP) model temperature and humidity vertical profiles to simulate 6.2 µm, 7.3 µm, 13.4 µm, 11 µm, and 12 µm cloud free and overcast radiances and brightness temperatures. For the simulation of cloudy radiances black-body clouds were inserted successively on each RTTOV vertical pressure levels. The appropriate cloud top is chosen as the value that gives the best fit to the simulated radiances (for AVHRR only based on the 11 µm channel).

Concerning the clouds that are labelled as semi-transparent by the cloud type method, two different approaches have now been followed. For NOAA AVHRR data, a histogram-based method (first introduced by Inoue, 1985, and further developed by Derrien and LeGleau, 1988), utilising the brightness temperature differences in the two infrared channels at 11 µm and 12 µm, has been used. The final implementation in the SAFNWC software is outlined by Korpela et al. (2001). For MSG SEVIRI data, the so called $H_2O$/IRW intercept method (Schmetz et al, 1993) and the radiance ratioing method (outlined by Menzel et al.,1983) has been used. Both methods utilise linear relationships between radiances in one window channel and in one sounding channel to estimate the cloud top.

Concerning the final CM-SAF product, cloud top information is expressed in three different ways:

- Cloud Top Temperature (CTT), expressed in Kelvin.
- Cloud Top Height (CTH), expressed in meters.
- The Cloud Top Pressure (CTP), expressed in pressure coordinates (hPa).

It is worth pointing out here that CTH is defined as the mean cloud altitude relative to the ground level (given by the GTOPO30 digital elevation model) and not to the sea level!

The final daily and monthly average products are calculated by averaging the original algorithm output in 1 km resolution over 15x15 km grid sub-areas. Cloud-top temperature and height are averaged linearly while cloud-top pressure is averaged logarithmically. Generally, for all products such pixels where the retrieval failed for any reason are excluded from averaging. Figure 5 below gives an example of the CTH product for April 2004.

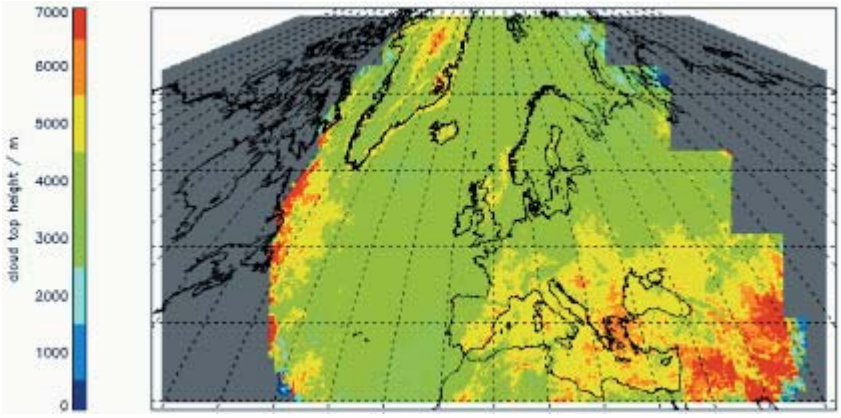


**Figure 5** Example of the CTH monthly mean product for April 2004.

The accuracy of this product is still under investigation, mainly because of a great lack of ground-based measurements to compare with. Generally, the method applied to opaque clouds have been shown to give reasonable estimations (although generally underestimating cloud top heights) while the method applied the semi-transparent correction of cloud heights has been noticed to give results with very variable quality. The latter method applied to NOAA AVHRR data has also been shown to fail when treating complex situations with multi-layered clouds. In such situations, the product will not be defined.

### *3.4 Cloud Phase (CPH)*

The present CPH product is based on a simple algorithm using only brightness temperatures measured at the infrared channel at 11 µm ($T_{11}$), i.e., a pure temperature interpretation approach is applied. This method is identical to the method used by the International Satellite Climatology Project (ISCCP, see Rossow and Schiffer, 1991).The cloud top is interpreted as consisting of pure ice particles if $T_{11}$ is lower than 233 K and by water particles if $T_{11}$ is higher than 260 K. In between, both cloud phases may co-exist (the mixed phase). The CPH product is given for each component in percent. The calculation of the average product is similar to the average cloud-type product as explained earlier.

Figure 6 below gives an example of the CPH product for the water cloud contribution for April 2004.

This product will be enhanced in the near future by adding a daytime algorithm linked with the radiative transfer calculations for retrieval of the cloud optical thickness product (COT - see next sub-section).

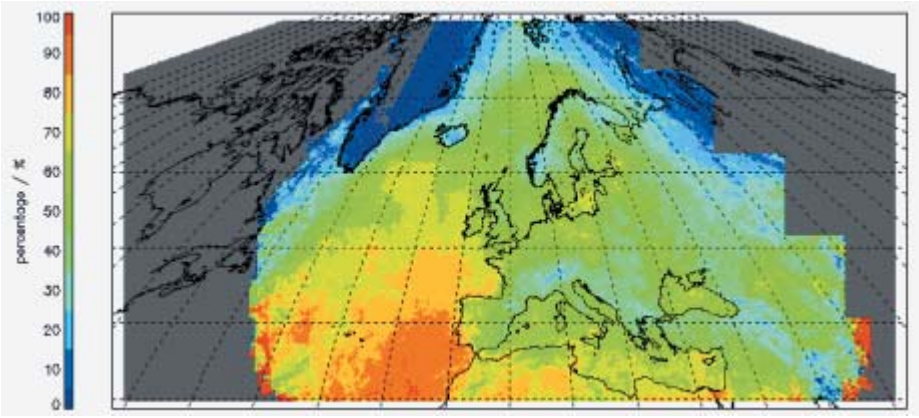


**Figure 6** Example of the CPH monthly mean product for April 2004 showing the contribution from water clouds.

### *3.5 Cloud Optical Thickness (COT)*

This product provides information on the Cloud Optical Thickness for pixels that are flagged cloudy by the cloud detection test (the cloud mask). The retrieval algorithm is based on 0.6 µm and 1.6 µm radiances of the NOAA AVHRR and MSG SEVIRI instruments. The algorithm retrieves also cloud droplet effective radius as an intermediate product.

The method to retrieve the cloud optical thickness utilizes solar reflected measurements at non-absorbing and absorbing wavelengths. The underlying principle of the method is that cloud reflectance at a non-absorbing channel in the visible wavelength region is primarily a function of the optical thickness, whereas reflectance at a water or ice absorbing channel in the near infrared is primarily a function of cloud particle size. By combining the information of non-absorbing and absorbing channels it is possible to retrieve the droplet effective radius and the cloud optical thickness. A Radiative Transfer Model (RTM), Spherical Harmonics Discrete Ordinate Model (SHDOM), is used to simulate cloud reflectance as a function of cloud optical thickness (Roebeling et al., 2001). With SHDOM (Evans, 1998) look up tables (LUT) of the top of the atmosphere reflectivity were generated for plane parallel clouds with different optical thicknesses, as a function of surface albedo, satellite zenith angle, solar zenith angle, relative azimuth angle and cloud thermodynamic phase. Because SHDOM is unstable for some cloud calculations it is being considered to replace these LUTs with Doubling-Adding KNMI (DAK) LUTs. The DAK radiative transfer model is developed for narrow band multiple scattering calculations at visible wavelengths in a homogeneous cloudy atmosphere (De Haan et al. 1987 and Stammes 2001).

Figure 7 below illustrates the LUT as resulting from the radiative transfer simulations for one specific viewing and illumination situation.

The final daily and monthly average product is calculated by logarithmic averaging of the original algorithm output in 1 km resolution over 15x15 km grid squares. Such pixels where the retrieval failed for any reason are excluded from averaging. Notice that the estimation of the COT product is possible only if visible imagery are available.

Figure 8 shows an example of the COT product for the month of April in 2004.

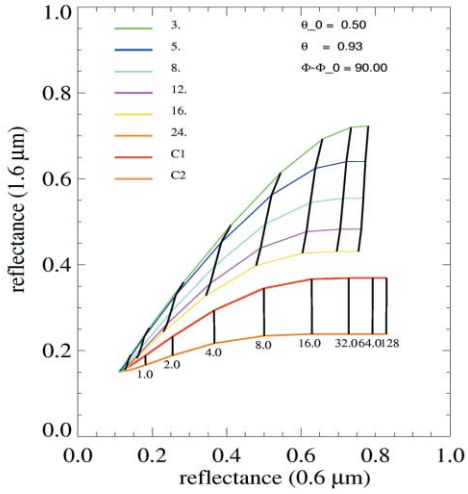


**Figure 7** The relationship between reflectivity at 0.6 and 1.6 µm for various classes of optical thickness and effective radius. The simulations were done for water and ice clouds using a specific geometrical case $(\theta=40,\ \theta_0=30,\ \phi=30)$.

Validation efforts so far have not been possible due to lack of appropriate ground measurements. But through the relation with the cloud liquid water path product (CWP – see sub-section 3.6) it is anticipated that the relative accuracy should lie within 20 %. It must be mentioned that the accuracy of the COT product decreases at very high COT values (i.e., the visible measurement is less correlated with COT values at high reflectivities). However, the most serious weakness of this product in its current version is the inability to compensate accurately for varying surface reflectivities. This means that in cases of semi-transparent clouds overlying surfaces with high surface reflectivities (e.g., thin Cirrus over the Greenland ice sheet) the optical depth will be largely overestimated. Future versions of this product will include improved compensations for varying surface reflectivities by use of surface reflectivity maps.

Lastly, currently there is no dependency between the CPH and COT products, i.e., the CPH product is not used when deriving COT. Instead, an internal interpretation of cloud phase is used for COT extraction. Later versions of the CPH and COT products will be consistent with each other.

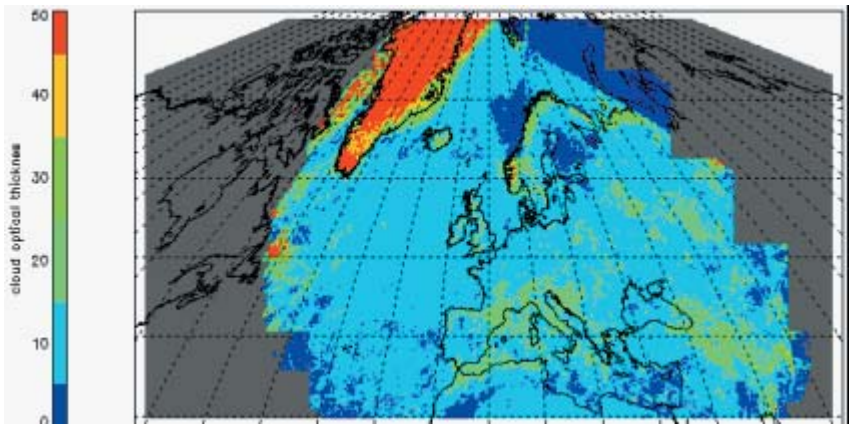


**Figure 8** Example of the COT monthly mean product for April 2004.

*3.6 Cloud Liquid Water Path (CWP)*

The Cloud Liquid Water Path (CWP) product is calculated as a function of the Cloud Optical Thickness and the estimated droplet effective radius. Note that for the current version of the product the CWP product does not include contributions from ice water or water vapour.

The method uses reflected solar radiation measurements at non-absorbing wavelengths and at water absorbing near infrared wavelengths to determine the optical thickness and the effective radius of clouds droplets (Han et al., 1995). The cloud liquid water path (CWP) may be derived with the cloud optical thickness and the droplet effective radius estimates which are calculated from the 0.63 and 1.6 micron channel data. The cloud liquid water path (CWP) may then be derived using the following equation (Stephens, 1984):

$$CWP = \frac{2}{3}.COT \ .r_e.\rho_l$$

where $\rho_l$ is the density of liquid water, $r_e$ is the droplet effective radius of water particles, which is a function droplet size distribution. The effective radius retrieved from the satellite data is based on the cloud top reflectivity at 1.6 µm.

Currently the Cloud Ice Water Path is not an output product. However, in the CWP maps an estimate of the Cloud Ice Water Path is made by assuming an effective radius or 30 micron for the small ice crystals and an effective radius of 40 micron for the large ice crystals. For later product versions, work is foreseen to derive an Ice Water Path (CIWP) product in a more sophisticated manner

The final daily and monthly average product is calculated by linear averaging of the original algorithm output in 1 km resolution over 15x15 km grid squares. Such pixels where the retrieval failed for any reason are excluded from averaging. As for the COT product, CWP retrievals are only possible in daylight situations.

Figure 9 shows an example of the CWP product for the month of April in 2004.

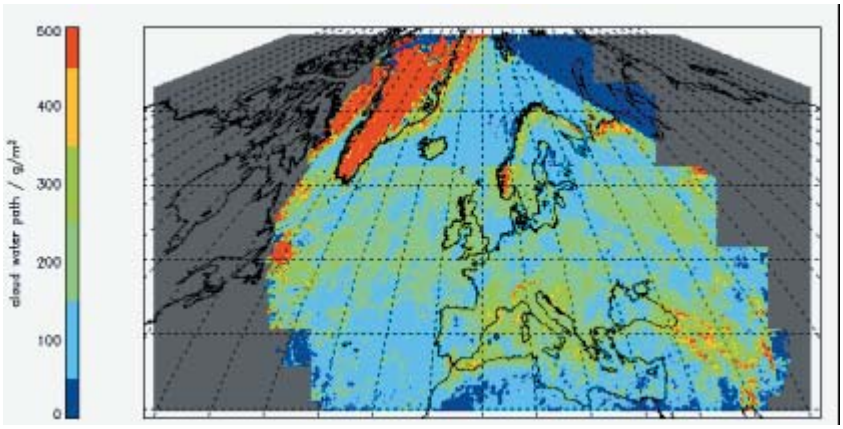


**Figure 9** Example of the CWP monthly mean product for April 2004.

The CWP is calculated from COT and droplet effective radius ($r_e$) information. Consequently the errors in the retrieved COT and $r_e$ will affect the CWP retrieval. This means that for clouds with COT > 50 the CWP retrievals will become less reliable. In addition, due to 3D cloud effects the droplet effective radius may be largely overestimated. The retrievals have shown that in these cases the CWP is largely overestimated. Recent validation activities based on ground based microwave radiometer measurements indicated a relative accuracy of 15 %.

## 4 Outlook for the future

During the period 2005-2007, some further development of cloud retrieval algorithms will take place (most of them already mentioned in previous sections). However, the most important goal is to make algorithms adapted for processing on a much larger geographical domain. By 2007 a system for running the polar satellite algorithms over the Inner Arctic region and the geostationary algorithms over the full MSG disk will be developed. Both these geographical areas are shown in Figure 1. This means that from the start of the Full Operations Phase of the Climate Monitoring SAF in 2007 climate products will be produced over this large geographical domain. To realise this, some effort is needed to guarantee the full access of the required data to achieve the desired geographical coverage. For example, a system for accessing and archiving NOAA HRPT data from several receiving stations at high latitudes is necessary in order to cover the inner Arctic region properly. On a longer time perspective (i.e., in the Full Operations Phase) cloud algorithms will be upgraded taking into account new approaches for improved cloud parameter retrieval. Revised results will be produced in connection to major reprocessing events.

***References***


De Haan, J. F., Bosma, P., and Hovenier, J. W., 1987: The adding method for multiple scattering calculations of polarized light, Astron. Astrophys., 183, 371-391.

Derrien, M. and H. LeGleau, 2003: SAFNWC/MSG SEVIRI cloud products, Proc. 2003 EUMETSAT Meterological Satellite Con ference, Weimar, Germany, 29 Sep – 3 Oct. 2003, EUM P 39, 191-198.

Dybbroe, A., Thoss, A. and Karlsson, K.-G., 2005: SAFNWC AVHRR cloud detection and analysis using dynamic thresholds and radiative transfer modelling – part I: Algorithm description, J. Appl. Meteor, Vol.44, No 1, pp. 39-54. (Paper 1)

Dybbroe, A., Thoss, A. and Karlsson, K.-G., 2005: SAFNWC AVHRR cloud detection and analysis using dynamic thresholds and radiative transfer modelling – part II: Validation, J. Appl. Meteor, Vol.44, No 1, pp. 55-71. (Paper 2)

Evans K.F., 1998: The Spherical Harmonics Discrete Ordinate, "Method for Three-Dimensional Atmospheric Radiative Trans fer", J. Atmos. Sci., 55, 429-446.

Eyre J., 1991, A fast radiative transfer model for satellite soundings systems. ECMWF Res.Dep.Tech.Mem 176. ECMWF, Reading, United Kingdom.

Han, Q., W.B. Rossow and A.A. Lasis, 1994: Near-Global Survey of Effective Droplet Radii in Liquid Water Clouds Using ISCCP Data, J. Climate, 7, 465-497.

Korpela, A., Dybbroe, A., and Thoss, A., 2001. Retrieving Cloud Top Temperature and Height in Semi-transparent and fractional cloudiness using AVHRR. NWCSAF Visiting Scientist Report. SMHI Reports Meteorology, 100, Available from SMHI, Folborgsvägen 1, SE-60176 Norrköping, Sweden.

Menzel, W.P., W.L. Smith and T.R. Stewart, 1983: Improved cloud motion wind vector and height assignment using VAS, J. Clim. Appl. Meteorol., 22, 377-384.

Roebeling R.A., D. Jolivet and A. Feijt, 2001: Cloud optical thickness and cloud liquid water path retieval from multi-spectral noaa-avhrr data, Proc. The 2001 EUMETSAT Meteorological Satellite Data User's Conference, Antalya, Turkey, 2001, 629-637.

Rossow, W.B. and R.A. Schiffer, 1991: ISCCP cloud data products. Bull. Amer. Met. Soc., 72, 2-20.

Saunders, R. W., Matricardi, M., and Brunel, P., 1999: An Improved Fast RadiativeTransfer Model for Assimilation of Satellite Radiances Observations. Quart. J. Royal Meteorol. Soc., 125, 1407.1425.

Stammes, P., 1994: Errors in UV reflectivity and albedo calculations due to neglecting polarisation, Proc. SPIE 2311, 227-235.

Stephens, G. L., 1984: The parameterization of radiation for numerical weather prediction and climate models, Mon.Wea. Rev., 112, 826-867.

Schmetz, J., K. Holmlund, J. Hoffman and B.Strauss, 1993: Operational cloud motion winds from Meteosat infrared images, J.Appl.Meteor, 32, 1207-1225